2026 IEEE/SICE International Symposium on System Integration (SII)
January 11-14, 2026. Cancún, México

Design of an Energy Efficient Electric Quadruped Robot based on Gravitationally Decoupled Actuation

Koichiro Moriwaki[1], Akifumi Okubo[1], Takahiro Aruga[1], Ryuichi Hodoshima[2], Takahiro Doi[3], and Gen Endo[1]

***Abstract*— Mammalian entertainment robots are popular for their friendly appearance, yet few achieve true legged locomotion due to high motor torque and power consumption requirements. In this study, we propose a mammalian electric quadruped walking robot employing Gravitationally Decoupled Actuation (GDA), which enables high-speed locomotion while minimizing the power required for walking. Using a dynamics simulator, we compared two configurations—conventional rotary joint actuation and the GDA model—and evaluated their motor torque and power requirements. Furthermore, based on commercial actuator specifications, we examined the feasibility of a practical GDA-based design. We also investigated a gravity compensation mechanism aimed at reducing motor peak torque and enabling long-duration operation. Simulation results showed that the GDA configuration reduced torque and power demand, achieving approximately 2.24 times the walking speed of the rotary joint actuation model under the same power limit. Introducing gravity compensation further reduced peak torque during the stance phase, making the system more suitable for prolonged operation.**

I. INTRODUCTION

Entertainment robots require not only a friendly appearance to attract customers but also high energy efficiency for long-duration operation. Furthermore, one example of entertainment robot configurations is the multi-legged robot, which enables dynamic and lively locomotion. The leg structures of multi-legged robots are generally classified into two main types: the mammalian type, in which the hip, knee, and ankle joints are arranged almost vertically beneath the body, and the reptilian type, in which the legs extend laterally from the body. In particular, mammalian robots are highly popular in applications such as amusement parks due to their approachable appearance. However, in many cases, wheels support the robot's weight, and examples of robots walking solely on legs are rare. For instance, the "Grand Éléphant" at the French theme park Les Machines de l'île [1] and Honda's two-wheeled mobility vehicle "Koraidon" [2] entertain visitors by providing a sense of presence through their friendly looks and movements. Nevertheless, both employ wheel-driven locomotion, with legs serving primarily decorative purposes. If walking using only legs becomes possible, it is expected that a deeper immersive experience can be achieved. In light of this background, this study focuses on mammalian walking robots and investigates efficient actuation methods.

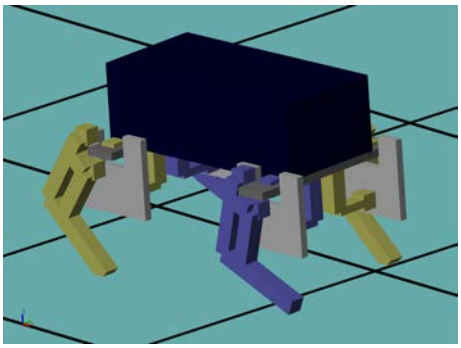

Fig. 1: GDA walking model on the dynamics simulator

In conventional mammalian robots, rotary joint actuation has been commonly adopted as the driving method. For example, Boston Dynamics' "Spot" employs rotary joint actuation [3]. However, this method requires large actuator output during walking, leading to challenges such as reduced walking speed and decreased energy efficiency. Therefore, this study adopts Gravitationally Decoupled Actuation (GDA) [4], which is considered effective in addressing these issues. GDA separates the leg motion into horizontal and vertical directions relative to the gravitational axis, allowing the actuators to independently control velocity and force components. Theoretically, this actuation method can achieve zero power consumption during horizontal locomotion while maintaining a constant center of mass height. There are several possible leg mechanism designs to achieve GDA; this study adopts a configuration where linear actuators are arranged in the horizontal and vertical directions, and their displacements are amplified by a pantograph mechanism. This configuration is expected to minimize the output power required for walking, improving energy efficiency and increasing walking speed.

Previous research on GDA includes the hydraulic-driven hexapod walking robot ASV (Adaptive Suspension Vehicle) by K. Waldron et al. [5] and the electric quadruped walking robot TITAN-IV by Yoneda et al. [6]. However, both of these feature either hexapod configurations or reptilian leg arrangements. To the best of our knowledge, there are no research examples applying GDA to electric quadruped walking robots with mammalian leg configurations.

Tsunoda et al. reported that, in static walking, the reptilian leg configuration consumes less power than the mammalian leg configuration [7]. Thus, in conventional discussions on locomotion efficiency, the reptilian configuration, where

[1] Koichiro Moriwaki, Akifumi Okubo, Takahiro Aruga, and Gen Endo are with the Department of Mechanical Engineering, Institute of Science Tokyo, 2-12-1 Ookayama, Meguro-ku, Tokyo 152-8552, Japan. moriwaki.k.45b7@m.isct.ac.jp

[2] Ryuichi Hodoshima is with the Graduate School of Science and Engineering, Saitama University, 255 Shimo-Okubo, Sakura-ku, Saitama-shi, Saitama 338-8570, Japan.

[3] Takahiro Doi is with the Department of Robotics, College of Information Science and Engineering, Kanazawa Institute of Technology, 7-1 Ohgigaoka, Nonoichi-shi, Ishikawa 921-8501, Japan.

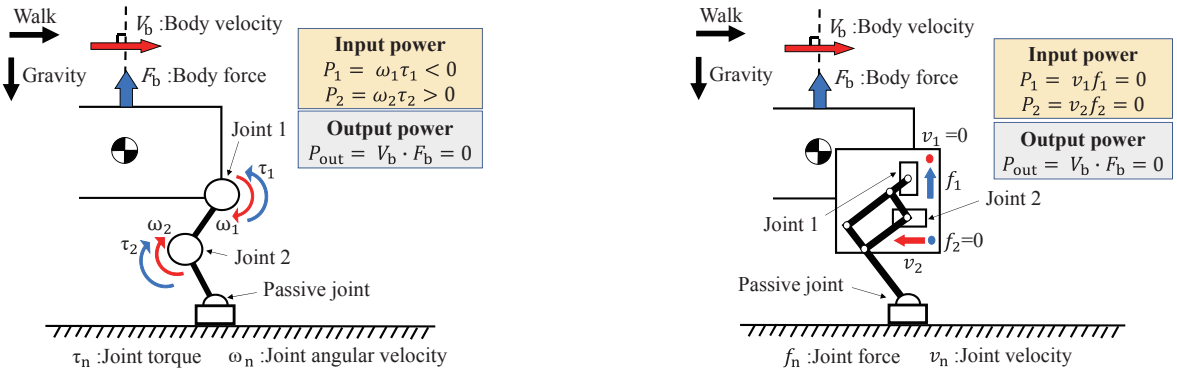

(a) Rotary joint actuation [8]

(b) Gravitationally decoupled actuation [8]

Fig. 2: Comparison between two actuation mechanisms

legs protrude laterally, has been considered advantageous. However, in applications such as entertainment robots that require a friendly appearance, the mammalian leg configuration tends to be preferred because, in addition to attracting visitors, setting the body position higher enables a more impressive presentation. Therefore, it is necessary to achieve high locomotion efficiency while adopting the mammalian configuration.

The GDA adopted in this study is not limited to the conventional reptilian leg configuration but allows a flexible design independent of the leg arrangement. In other words, the leg morphology (mammalian or reptilian) and the actuation method (GDA) are independent design elements, and their combination enables the realization of an electric quadruped robot with a mammalian leg configuration applying GDA. If a mammalian electric walking robot utilizing GDA is achieved, the required power can be significantly reduced compared to conventional rotary joint actuation, enabling both improved locomotion efficiency and higher speed.

Based on the above, this study aims to design a mammalian electric quadruped walking entertainment robot applying Gravitationally Decoupled Actuation (GDA) to achieve both high-speed and efficient locomotion. Using a dynamics simulator, two mammalian models—the rotary joint actuation model and the GDA model (Fig. 1)—are compared. The effectiveness of GDA is verified from the perspective of required motor torque and power (mechanical work) through actuator output comparison. Furthermore, the feasibility of practical implementation is investigated based on commercial electric actuator product specifications, and the effect of peak torque reduction by introducing a gravity compensation mechanism is also evaluated with the aim of enabling long-duration operation.

II. Efficiency and Speed Improvement of Walking Using Gravitationally Decoupled Actuation

A. Conventional leg actuation using rotary joints

In this section, we describe conventional leg actuation using rotary joints (Rotary joint actuation). Consider a walking robot with negligible leg mass, shown in Fig. 2a, moving at a constant speed on a flat horizontal surface without vertical displacement of its center of mass. In this case, the ground reaction force F_b supporting the weight of the robot at the foot and the robot's velocity V_b are orthogonal to each other. Therefore, the output power is zero, and theoretically, no energy is required.

However, in rotary joint actuation, both velocity and force are generated simultaneously, causing positive and negative input power exchange between actuators ($P_1 < 0$ W, $P_2 > 0$ W) At present, compact regenerative devices suitable for robotic applications have not yet been realized, and all transferred power is dissipated as thermal energy. As a result, this leads to a decrease in energy efficiency during walking. Such loss is inherent to rotary joint configurations and cannot be avoided even under appropriate control. In addition, the excessive power requirement and insufficient output relative to the target speed cause a reduction in the robot's locomotion speed.

B. Gravitationally Decoupled Actuation Using Linear Joints

In this section, we describe Gravitationally Decoupled Actuation (GDA), which effectively addresses the problems of conventional rotary joint actuation. The GDA shown in Fig. 2b employs linear actuators arranged horizontally and vertically relative to the gravitational direction, combined with a pantograph mechanism. This setup allows each actuator to generate either velocity or force independently, theoretically reducing the input power to the actuators during walking to zero (P_1 = 0 W, P_2 = 0 W) [9]. As a result, unnecessary power exchange between actuators is eliminated, leading to improved energy efficiency. Furthermore, by preventing excessive power generation, higher walking speeds become achievable. On the other hand, when operating on sloped or uneven terrain, the orthogonality between the gravitational and actuation directions is compromised, preventing the decoupling of force and velocity in each actuator and potentially reducing locomotion efficiency. However, since the entertainment robot targeted in this study is primarily intended to operate in theme-park environments where steep slopes are avoided and the ground is generally flat and well maintained, the GDA mechanism is considered to be highly compatible with such applications. For example, according to the 2010 ADA Standards for Accessible Design and Japan ' s Universal Design Guidelines for Expo 2025, slopes of 1:20 (approximately 2.86 °) or less are recommended for barrier-free accessibility [10] [11]. For these reasons, this mechanism is adopted in this study.

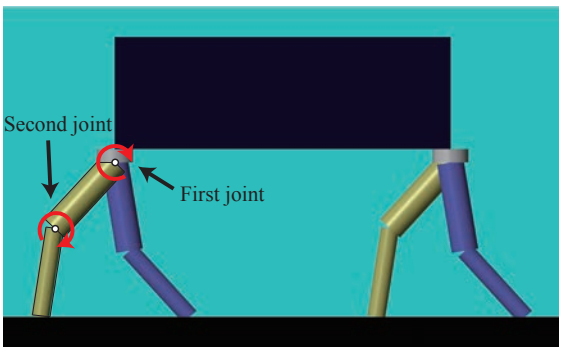

(a) Rotary joint actuation walking model

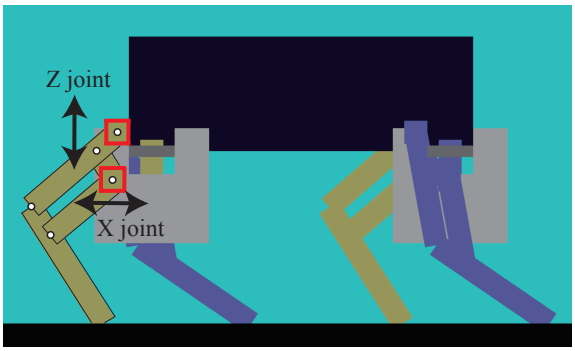

(b) GDA walking model

Fig. 3: Comparison between rotary joint actuation walking model and GDA walking model

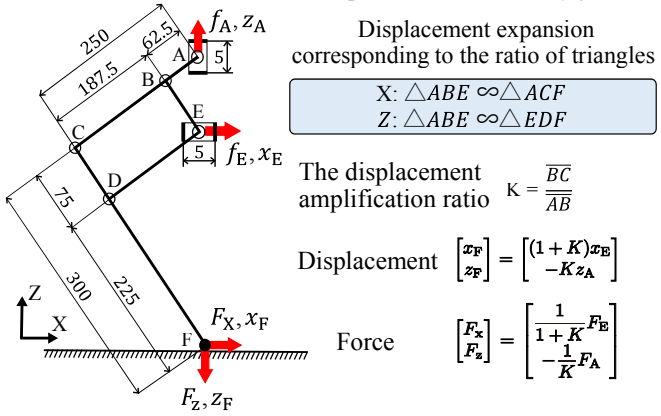

Fig. 4: GDA link length and input-output relationship between actuator and foot tip

III. Comparative Study of Two Mammalian Configurations Using a Dynamics Simulator

Using MATLAB/Simulink, two quadruped walking robots with mammalian leg configurations were constructed: the rotary joint actuation model (Fig. 3a) and the Gravitationally Decoupled Actuation (GDA) model (Fig. 3b). This dynamic simulator can calculate the motor torque and rotational speed required for walking. Using this simulator, the actuator outputs of both configurations are compared and evaluated during trot gait.

A. Specifications of the Dynamics Simulator

Common specifications for both robots are as follows: the torso dimensions are width 0.75 m, height 0.25 m, and depth 0.35 m; the total robot weight is 125 kg (torso 105 kg, each leg 5 kg). Walking conditions are set with a period of 1 s, forward speed of 0.335 m/s, and torso height (distance from the ground to the bottom of the torso) of 0.375 m. The swing leg trajectory follows a cycloid path, with a swing height of 0.05 m and a stride length of 0.335 m. The walking pattern is trot gait with a duty ratio of 0.5. Additionally, the forward direction of the robot is defined as the X-axis, and the vertical upward direction as the Z-axis, which will be used in the following discussion. In this study, to simplify the analysis, motions in the pitch and roll directions are assumed negligible, and evaluation focuses only on forward motion. Accordingly, degrees of freedom in pitch and roll are constrained with respect to the robot posture. In the rotary joint actuation model shown in Fig. 3a, the joints are defined sequentially from the leg root as the first and second joints. Regarding the leg mass distribution, the leg mass is allocated proportionally to the length of the two actively driven links. Here, the link length from the first joint to the second joint is set to 0.2 m, and the link length beyond the second joint is also set to 0.2 m. Next, in the GDA model shown in Fig. 3b, the linear actuators enclosed by red squares are assumed to consist of a motor and a ball screw. These linear actuators drive the pantograph mechanism. The actuator moving in the X-direction is defined as the X-joint, and the actuator moving in the Z-direction is defined as the Z-joint. For the leg mass distribution, the total leg mass is distributed proportionally to the length across the six driven links and linear components. The dimensional data of these links and linear parts are shown in Fig. 4.

Furthermore, as shown in Fig. 4, the pantograph mechanism employed in the GDA model amplifies the displacements of the X- and Z-joints at the leg tip based on the displacement amplification ratio K, which is determined by the geometric configuration of the links. In this configuration, joint displacement and output force are inversely related. In this study, the displacement amplification ratio K is set to 3. This mechanism allows the actuators to be concentrated near the center of the body, contributing to the weight reduction of the distal leg. Moreover, increasing the displacement amplification ratio narrows the distance between the parallel links, enabling an appearance similar to the thigh of a mammal.

B. Comparison of Torque Requirements for Rotary Joint Actuation and GDA model

The time histories of torque and rotational speed as virtual motor outputs are compared for two models of mammalian leg mechanisms. Figs. 5 and 6 show the torque and rotational speed variations of the motor output for each configuration, respectively. In these plots, the periods when the leg is off the ground (swing phase: red) and when it is in contact with the ground (stance phase: blue) are distinguished. To facilitate comparison of torque and rotational speed changes, the gearhead reduction ratio and ball screw lead were adjusted so that the motor's maximum rotational speed during the swing phase was approximately 5000 rpm. Note that the transmission efficiencies of the ball screw and gearhead are not considered here.

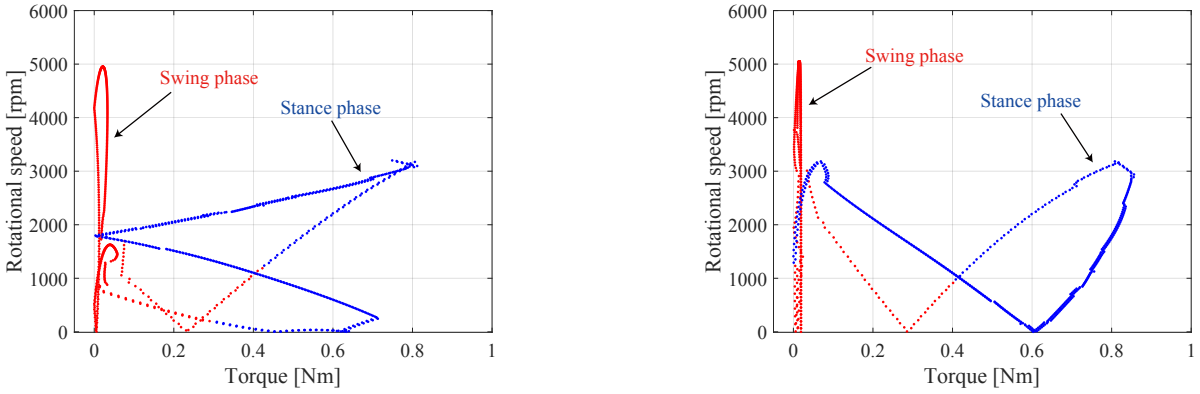

(a) First joint output **(b)** Second joint output

Fig. 5: Rotary joint actuation output (Rotational motor output)

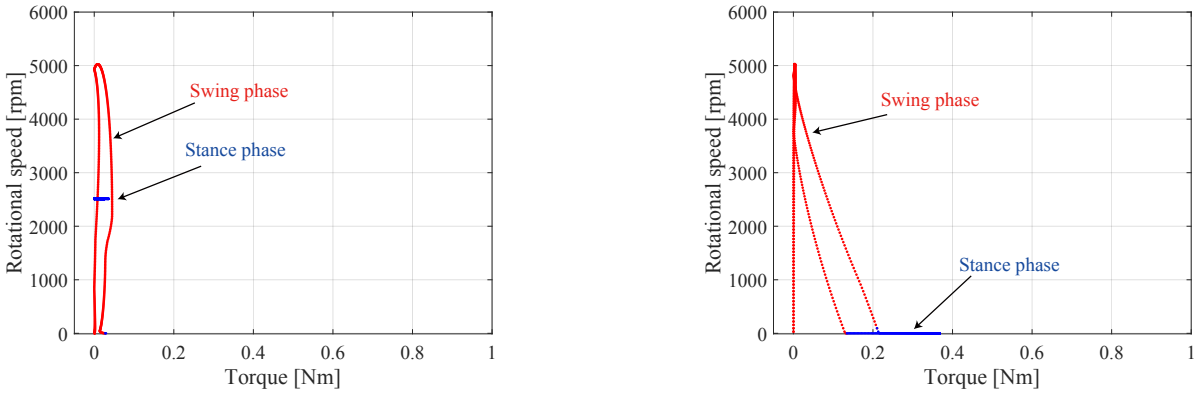

(a) X joint output **(b)** Z joint output

Fig. 6: GDA output (Rotational motor output embedded within the linear actuator)

The simulation results for the rotary joint actuation model are shown in Fig. 5. Figs. 5a and 5b illustrate the time histories of the virtual motor outputs (torque and rotational speed) at the first and second joints, respectively. A gearhead with a reduction ratio of 100 is assumed for both joint motors. As a result, the maximum torque during the stance phase at the first joint was calculated as 0.81 Nm, and 0.86 Nm at the second joint. Furthermore, both torque and rotational speed occurred simultaneously during the stance phase, indicating an increase in motor output power.

Next, the simulation results for the GDA model are shown in Fig. 6. Figs. 6a and 6b illustrate the transitions of the virtual motor outputs (torque and rotational speed) of the actuators in the X- and Z-directions, respectively. Here, the motor output inside the linear actuators (ball screw and gearhead) was evaluated. In this configuration, the lead of the ball screw (linear travel per one rotation) was set to 20 mm for each direction, and the gearhead reduction ratio was set to 5 in the X-direction and 16 in the Z-direction. Under these conditions, the maximum torque of the X-direction motor during the swing phase was 0.04 Nm, while that of the Z-direction motor during the stance phase was 0.37 Nm. Additionally, in the GDA model, either the rotational speed or torque was predominantly generated in each actuator, confirming that the generation of force and velocity is structurally separated. This characteristic arises from the structural design of the GDA mechanism and indicates that the simulation model appropriately reproduces this feature.

From these results, comparing the motor torque and rotational speed on the input side of the reduction gear in both configurations, it became clear that even under the same walking conditions with a mammalian leg configuration, the GDA model requires smaller torque compared to the rotary joint actuation model. Since actuators that can be mounted on an actual machine have upper limits on output torque, configurations like the GDA that can reduce torque requirements are shown to be extremely effective leg mechanisms for practical implementation.

IV. Verification of the Actual System Configuration Feasibility Using Commercial Product Specifications

A. Verification of actuator configuration based on commercially available electric component specifications

With a view toward the future practical development of an electrically driven mammalian GDA robot, this study investigates whether the GDA mechanism can be constructed using commercially available electric components. The validity of the actuator configuration was evaluated through simulations based on selected product specifications, assuming a practical system setup. Each actuator consists of a ball screw and a gearhead. The ball screw lead and gearhead reduction ratio are set to 30 mm and 4.3 in the X-direction, and 5 mm and 4.3 in the Z-direction, respectively. The torque transmission

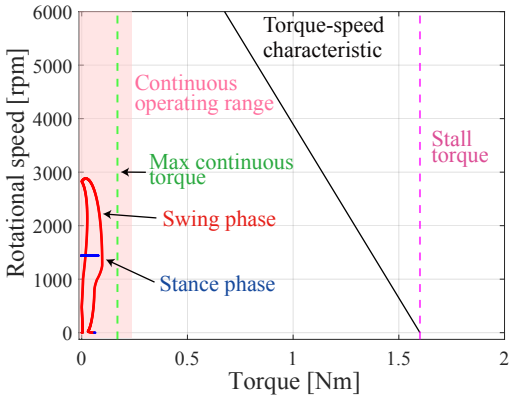

(a) X motor output

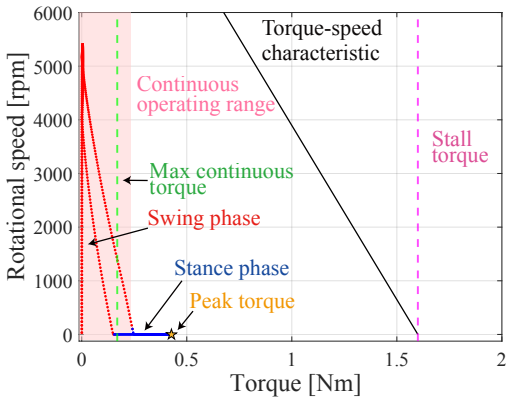

(b) Z motor output (No gravity comp.)

Fig. 7: GDA output incorporating actual product specifications (Rotational motor output embedded within the linear actuator)

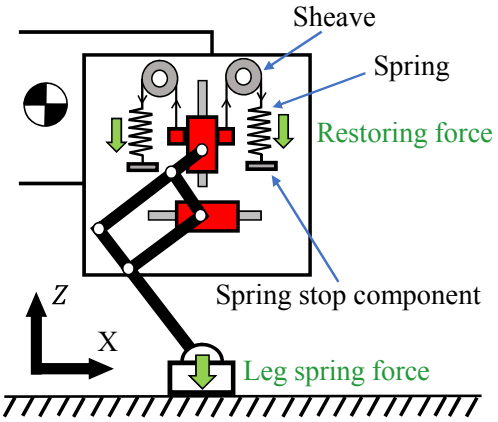

Fig. 8: Gravity compensation mechanism layout diagram

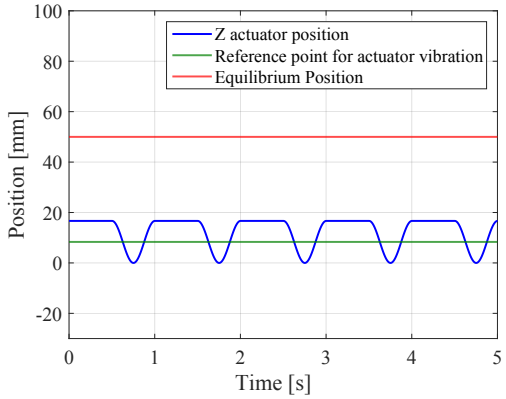

Fig. 9: Z actuator position

efficiency of both components is assumed to be 0.9. Suitable commercial products were selected to ensure axial thrust and maximum load torque remain within allowable limits. For the motor, torque–speed characteristics, winding resistance, and continuous operating range were considered. Consequently, a Maxon Japan BLDC motor (EC45 BL D 150 W KL 2WE A), rated at 150 W and 48 V, was employed. Regarding the indicators shown in Fig. 7, the pink dotted line represents the stall torque of 1.6 Nm; the black solid line connects the stall torque point (1.6 Nm, 0 rpm) and the maximum continuous operating output point (0.169 Nm, 9290 rpm); the green dotted line indicates the maximum continuous torque of 0.169 Nm; and the light red band represents the continuous operating range (up to 0.234 Nm) calculated from winding resistance, copper loss, and torque constant.

A simulation of one gait cycle was performed using this configuration, and the time histories of torque and rotational speed in the X- and Z-direction actuators are shown in Figs. 7a and 7b, respectively. The simulation results confirmed that, although the torque of the Z-direction actuator during the stance phase exceeded the continuous operating range at certain points, the peak torque (indicated by stars in Fig. 7b) remained below the stall torque. These results demonstrate that even with a mammalian leg arrangement employing GDA, a practical system configuration utilizing commercially available electric components is feasible.

B. Verification of the load distribution effect by introducing the gravity compensation mechanism

The results of the previous section indicate that the peak torque during the stance phase may exceed the motor's continuous operating range. Since electric motor drives generally have greater output limitations than hydraulic systems, poses a significant concern for applications requiring prolonged continuous operation, such as entertainment robots. Accordingly, it is essential to address the following issues: suppressing current increases caused by excessive torque and ensuring that the peak torque during the stance phase remains within the continuous operating range. To satisfy these requirements, this paper proposes introducing a gravity compensation mechanism aimed at reducing the peak torque generated during the stance phase.

The goal of this study was to keep the motor torque during the stance phase as much as possible within the continuous operating region by using a compensation method with a linear spring. As shown in Fig. 8, this mechanism is assumed to consist of two springs connected in parallel to the Z-direction actuator. In the MATLAB/Simulink environment, the gravity compensation mechanism was modeled by defining the spring constant and neutral point within the linear joint configuration of the Z-direction actuator. The strain energy stored in the spring is conserved without damping. For the spring constant and neutral point position, product specifications from Tokyo Spring Manufacturing Co., Ltd.'s

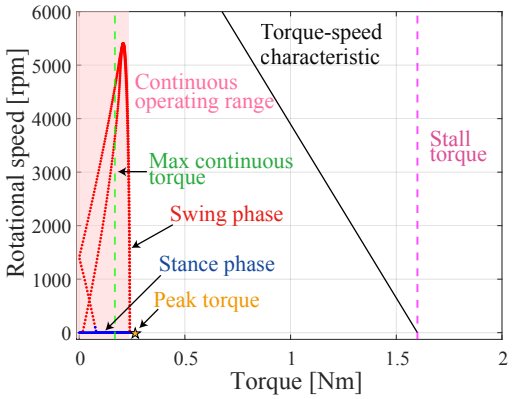

Fig. 10: Z motor output (Gravity comp.)

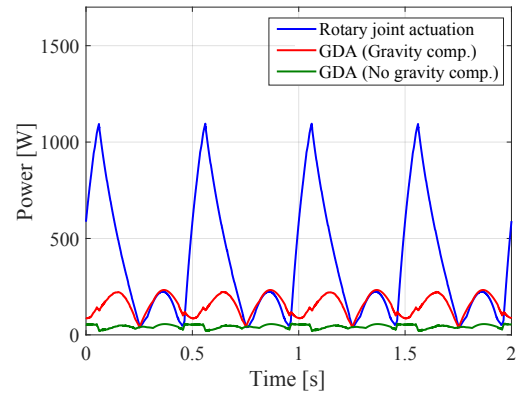

(a) Power compare

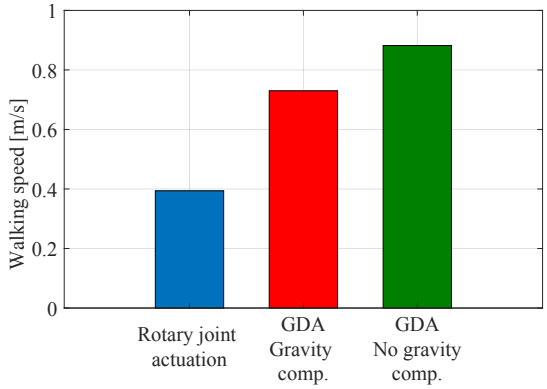

(b) Speed compare

Fig. 11: Comparison of power consumption with and without output spring

Light Load TL20 × 125 was used. This choice aimed to closely approach the target continuous operating range. The product specifications are as follows: free length 125 mm, outer diameter 20 mm, spring constant 10.69 N/mm, and maximum allowable deflection 50 mm. Furthermore, this product's dimensions are physically compatible for installation on the robot under development. Fig. 9 shows the displacement of the Z-actuator during walking. The actuator exhibits periodic motion with an amplitude of 8 mm, referenced from the green line. The neutral point (red line) is set 50 mm above the lowest point of the Z-direction stroke during walking, and it is connected at the spring mounting endpoint (blue line), ensuring the spring is always stretched opposite to the self-weight direction.

The simulation result is shown in Fig. 10. From this result, the peak torque during the stance phase was 0.42 Nm without gravity compensation (Fig. 7b), whereas it was reduced to 0.26 Nm with gravity compensation. On the other hand, the torque during the swing phase tended to increase due to the elastic force of the spring in the gravity compensation mechanism. However, considering these effects, the peak torque over the entire walking cycle was observed to be reduced compared to the case without gravity compensation. These results demonstrated that introducing a gravity compensation mechanism reduced peak torque during the stance phase and concentrated the torque–speed distribution within the continuous operating range, enabling a robot configuration suitable for long-duration operation.

C. Comparison of Required Power and Walking Speed

For the three configurations—rotary joint actuation, GDA without gravity compensation, and GDA with gravity compensation—we calculated and compared the total mechanical power output of the actuators across all four legs. Simulations were conducted under identical walking conditions for all configurations, as in the previous section.

Fig. 11 summarizes the results. As shown in Fig. 11a, the maximum total power was 1095.5 W for the rotary joint actuation model and 59.0 W for the GDA model without gravity compensation. When the gravity compensation was applied to the GDA model, power consumption during the swing phase increased, resulting in a total power of 232.9 W, which remains substantially lower than that of the rotary joint actuation model.

Next, we evaluated the achievable walking speeds under actuator power limitations, as illustrated in Fig. 11b. Assuming a total actuator power limit of 700 W and a unified stride length of 0.335 m, the walking period was adjusted to equalize total output across configurations. Under these conditions, the rotary joint actuation model achieved a speed of 0.394 m/s with a cycle period of 1.85 s. The GDA model without gravity compensation reached 0.882 m/s with a cycle period of 0.38 s, while the GDA model with gravity compensation achieved 0.730 m/s with a cycle period of 0.46 s. Thus, at the same power limit, the GDA configurations demonstrated superior speed performance, attaining approximately 2.24 times (without gravity compensation) and 1.85 times (with gravity compensation) the speed of the rotary joint actuation model.

These results indicate that, even under identical actuator output constraints, the GDA configuration converts output power into walking speed more efficiently than the rotary joint actuation model. Therefore, implementing GDA in mammalian leg robots is an effective design strategy for achieving high-speed locomotion within realistic actuator power limits.

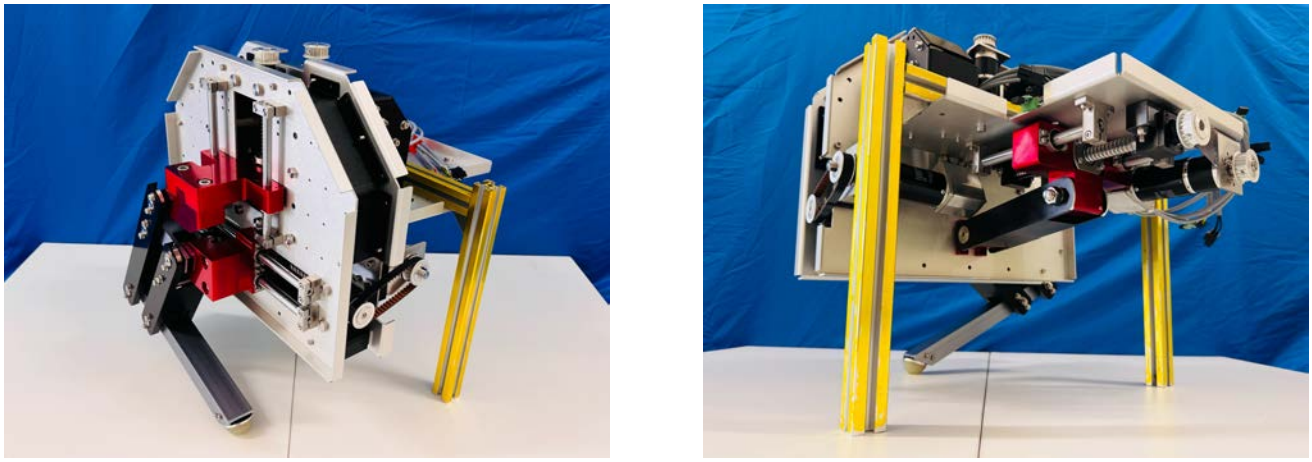

(a) Front angle **(b)** Back angle

Fig. 12: Single-leg test rig

V. CONCLUSIONS

In this study, the performance of two mammalian leg configurations—the rotary joint actuation model and the Gravitationally Decoupled Actuation (GDA) model—was compared using a dynamic simulator. Their effectiveness was evaluated in terms of output torque and required power, and feasibility studies were conducted based on commercially available component specifications. In addition, the effect of a gravity compensation mechanism for reducing peak torque to enable long-duration operation was investigated. The results show that the GDA configuration improves both energy efficiency and walking speed by reducing the required power, even in electric drive systems. This finding demonstrates that not only the laterally sprawling reptilian leg configuration—conventionally regarded as superior in locomotion efficiency—but also mammalian leg configurations can achieve high efficiency. Furthermore, the introduction of the gravity compensation mechanism was shown to reduce the peak torque during the stance phase and to concentrate the torque–speed distribution within the continuous operating range, thereby enabling a robot configuration suitable for long-duration operation.

Nevertheless, the GDA approach also entails drawbacks: constraining motion increases drivetrain complexity, which in turn raises the number of components, system weight, and overall cost.

As shown in Fig. 12, a single-leg test rig was fabricated, and we confirmed that each actuator operated properly and could drive the leg as designed. Furthermore, by performing a standing-up motion, we verified that the rig could lift its own weight. These results demonstrate that the basic functionality of the system has been validated and that it is ready for experimental evaluation. In future work, this test rig will be used to experimentally validate the findings obtained in this study. Specifically, quantitative evaluations will be conducted not only on practical aspects, such as actual power consumption and the effects of the gravity compensation mechanism, but also on trade-offs involving negative factors, including increased weight. Furthermore, design optimizations to mitigate these drawbacks will be examined, and the usefulness of GDA will be evaluated by comparing it with the rotary joint actuation model.

REFERENCES

[1] Les Machines de l'île, "Les Machines de l'île de Nantes," [Online]. Available: https://www.lesmachines-nantes.fr/ [Accessed: Aug. 5, 2025].

[2] Honda Motor Co., Ltd., "Honda Koraidon," [Online]. Available: https://global.honda/jp/motorcycle/brand/koraidon/ [Accessed: Aug. 8, 2025].

[3] Boston Dynamics, "Spot – Agile Mobile Robot," [Online]. Available: https://www.bostondynamics.com/products/spot [Accessed: Aug. 5, 2025].

[4] S. Hirose, Y.Umetani, "Leg Morphology and Mobility Characteristics of Walking Robots", Biomechanics, vol.5, pp.242-250, 1980.

[5] Waldron, Kenneth J. et al., "Configuration Design of the Adaptive Suspension Vehicle." The International Journal of Robotics Research 3, pp.37-48, 1984.

[6] K. Yoneda and S. Hirose, "Dynamic and static fusion gait of a quadruped walking vehicle on a winding path, "Proceedings 1992 IEEE International Conference on Robotics and Automation, Nice, France, vol.1, pp.143-148, 1992.

[7] S. Tsunoda, H. Nabae, K. Suzumori and G. Endo, "Power Consumption Comparison Between Mammal-Type and Reptile-Type Multi-Legged Robots During Static Walking," 2022 IEEE/SICE International Symposium on System Integration (SII), Narvik, Norway, 2022, pp. 459-466, doi: 10.1109/SII52469.2022.9708790.

[8] S. Hirose et al., "Quadruped walking robots at Tokyo Institute of Technology," in IEEE Robotics & Automation Magazine, vol. 16, no. 2, pp. 104-114, June 2009, doi: 10.1109/MRA.2009.932524.

[9] K. Nagatani (Ed.), G. Ishigami, D. Endo, K. Nagaoka, G. Endo, R. Hodoshima, S. Kamekawa, and M. Tanaka, "Rough Terrain Mobile Robotics", Tokyo, Japan: Corona Publishing, 2023, ch. 2, pp. 97-108.

[10] U.S. Department of Justice, "2010 ADA Standards for Accessible Design," 2010. [Online]. Available: https://www.ada.gov/law-and-regs/design-standards/2010-stds/ [Accessed: Aug. 5, 2025].

[11] Japan Association for the 2025 World Exposition, "Universal Design Guidelines for Facility Implementation," Jun. 2023. [Online]. Available: https://www.expo2025.or.jp/wp/wp-content/uploads/230613_02_01_Universal-Design-Guidelines.pdf [Accessed: Aug. 5, 2025].